

Desorption From Interstellar Ices

J. F. Roberts^{*}, J. M. C. Rawlings, S. Viti and D. A. Williams

Department of Physics & Astronomy, University College London, Gower Street, London WC1E 6BT

30 October 2018

ABSTRACT

The desorption of molecular species from ice mantles back into the gas phase in molecular clouds results from a variety of very poorly understood processes. We have investigated three mechanisms; desorption resulting from H₂ formation on grains, direct cosmic ray heating and cosmic ray induced photodesorption. Whilst qualitative differences exist between these processes (essentially deriving from the assumptions concerning the species-selectivity of the desorption and the assumed threshold adsorption energies, E_t) all three processes are found to be potentially very significant in dark cloud conditions. It is therefore important that all three mechanisms should be considered in studies of molecular clouds in which freeze-out and desorption are believed to be important.

Employing a chemical model of a typical static molecular core and using likely estimates for the quantum yields of the three processes we find that desorption by H₂ formation probably dominates over the other two mechanisms. However, the physics of the desorption processes and the nature of the dust grains and ice mantles are very poorly constrained. We therefore conclude that the best approach is to set empirical constraints on the desorption, based on observed molecular depletions - rather than try to establish the desorption efficiencies from purely theoretical considerations. Applying this method to one such object (L1689B) yields upper limits to the desorption efficiencies that are consistent with our understanding of these mechanisms.

Key words: astrochemistry – molecular processes – stars:formation – ISM: abundances – ISM: dust – ISM: molecules.

1 INTRODUCTION

In cold dark interstellar clouds, heavy molecules accumulate onto dust grains, forming icy mantles on their surfaces. This process, known as freeze-out, occurs on a timescale of a few times $10^9 n_H^{-1}$ years (where $n_H = n(\text{H}) + 2n(\text{H}_2)$ is the total hydrogen nucleon number density) in the absence of desorption. This is much less than the expected lifetime of a typical molecular cloud so, if freeze-out was unlimited, we would expect the majority of observations to show no evidence for heavy gas phase species. However, observations of molecules such as CO in dark clouds, for example L1689B, TMC1-CP and L134N (Lee et al. 2003; Smith et al. 2004; Wakelam et al. 2006), indicate that desorption processes must be operating for mantle growth to be limited.

Although this conclusion has been accepted for over 20 years, it is still not fully understood how this desorption occurs. Many possible mechanisms have been proposed, most of which require impulsive heating of grains

which can be caused by (a) direct impact of cosmic rays (Hasegawa & Herbst 1993; Hartquist & Williams 1990; Léger et al. 1985), (b) X-rays (Léger et al. 1985), (c) ultra-violet photons induced by cosmic rays (cosmic ray photodesorption) (Hartquist & Williams 1990; Duley et al. 1989), or (d) exothermic reactions occurring on the grain surface (Allen & Robinson 1975; Garrod et al. 2007), in particular the formation of molecular hydrogen (Willacy et al. 1994a; Duley & Williams 1993). Molecules can either be desorbed by classical evaporation (Léger et al. 1985) or by chemical explosions (Shen et al. 2004; Shalabiea & Greenberg 1994; Léger et al. 1985). These chemical explosions can only occur if the mantle has previously been irradiated with ultra-violet radiation which creates radicals. If the grain temperature is raised to ~ 27 K, the radicals become mobile and then undergo explosive reactions capable of expelling the entire grain mantle. We will not consider chemical explosions in this paper because in dark clouds with $A_V > 5$ magnitudes it is unlikely that the grain mantles will have received sufficient UV irradiation (Léger et al. 1985), and any radicals that do form are likely to be hydrogenated due to the high abundance of hydrogen atoms present (Willacy & Millar 1998).

^{*} E-mail: jfr@star.ucl.ac.uk

Recent chemical models of dark clouds tend to include only desorption via thermal evaporation (which is negligible for dark clouds with temperatures of 10 K) and/or direct heating by cosmic rays, using the formulation given by Hasegawa & Herbst (1993) (hereafter HH93) (Ruffle & Herbst 2000; Roberts et al. 2004). This paper, therefore, aims to test the assumption that desorption via direct cosmic ray heating is the only effective non-thermal desorption mechanism relevant to dark molecular cores. In this study we adopt the model of a molecular cloud as being composed of an ensemble of dense (dark) cores in a more diffuse background (Garrod et al. 2006). Ices are probably only present in the cores. We set out to test the desorption efficiencies, by including in an existing model of dark cloud chemistry three desorption mechanisms (desorption resulting from H₂ formation on grains, direct cosmic ray heating and cosmic ray photodesorption) that have been formulated in the literature, to find their relative importance in dark cores. We believe these three mechanisms are likely to be the most important in this situation, in the absence of any nearby X-ray sources in the molecular cloud.

We note that there already exist several other studies which model these three desorption mechanisms, for example Willacy et al. (1994b) (hereafter WRW94) performed a study very close to our own. However, our work differs to that of WRW94 because we try to take a simpler approach; by modelling a static cloud rather than a collapsing one we can easily see the effects of adding desorption to our chemical model. We also look further into the assumptions made about the ability of each desorption mechanism to desorb molecules with higher adsorption energies, such as H₂O and NH₃ (Section 4.3). Most importantly, we attempt to constrain the efficiency of each mechanism by comparing our results to observations of CO depletion in star-forming regions.

The paper is structured as follows: In Section 2 we give a brief summary of these desorption mechanisms and in Section 3 we describe the model. The results are given in Section 4, and are discussed by comparing them to existing models in Section 5 and observations in Section 6. Concluding remarks are given in Section 7.

2 DESORPTION MECHANISMS

2.1 Desorption resulting from H₂ formation

It has long been suggested that the energy released from exothermic reactions on grain surfaces can release energy capable of desorbing mantle species (Allen & Robinson 1975). In particular, laboratory experiments on graphite substrates suggest that a non-negligible fraction, perhaps up to 40% (Creighan, Perry & Price 2006), (F. Islam, private communication) of the ~ 4.5 eV released in the surface formation of molecular hydrogen is transferred to the grain surface. This leads to local heating which may thermally desorb weakly bound mantle species (Duley & Williams 1993), although the extent to which the temperature rises transiently is not well determined, and depends on the local conductivity. In amorphous materials, the temperature rise may be relatively large.

Such a process may be *selective*, depending on the tem-

perature achieved as a result of the energy deposition. In previous work (Duley & Williams 1993; Willacy et al. 1994a,b), the conservative assumption was made that only the most volatile species (such as CO, N₂, NO, O₂, C₂ and CH₄) would be desorbed during the transient heating, corresponding to a threshold adsorption energy of $E_t = 1210$ K. Initially, we shall adopt the same threshold and range of volatile species, but we shall also consider the effects of variations from that value in Section 4.3.

The rate of desorption by this process for species i is given by:

$$R_{\text{hf}} = \varepsilon R_{\text{H}_2} M_s(i, t) \quad \text{cm}^{-3} \text{ s}^{-1} \quad (1)$$

where R_{H_2} is the rate of H₂ formation on grains. R_{H_2} is proportional to the available grain surface area and the sticking/reaction probability to form H₂ and is empirically constrained (at T=10 K) to be given by:

$$R_{\text{H}_2} = 3.16 \times 10^{-17} n(\text{H}) n_{\text{H}} \quad \text{cm}^{-3} \text{ s}^{-1} \quad (2)$$

where $n(\text{H})$ is the number density of atomic hydrogen and n_{H} is the total hydrogen nucleon density. $M_s(i, t)$ is the fraction of the mantle consisting of species i , calculated self-consistently as a function of time. ε is an efficiency parameter such that $\varepsilon M_s(i, t)$ gives the number of molecules of species i desorbing per H₂ molecule formed. The efficiency of this process is uncertain, but we can make a rough upper estimate as follows: If we assume that 40% (~ 2 eV) of the energy released during each H₂ formation is transferred to the grain, and given that the adsorption energies of the species we consider are ~ 1000 K ($\sim 8.2 \times 10^{-2}$ eV), we would expect that a maximum of ~ 20 molecules could be desorbed every time an H₂ molecule is formed. It is likely, however, that this process is less efficient, because such a high value for ε would prevent the build-up of any mantle material until very late times (Willacy & Millar 1998). We therefore run our model with values of ε ranging from 0.01 to 1.0, and present results for $\varepsilon = 0.01$ and 0.1.

2.2 Desorption by direct cosmic ray heating

In this paper, the rate of desorption by direct cosmic ray heating is calculated by simply considering the number of molecules capable of being desorbed per cosmic ray impact. This rate is different to that adopted in other models (see the discussion in Section 5.4).

As with desorption via H₂ formation, this process is believed to be selective (Willacy et al. 1994b), so only the volatile species (CO, etc.) are expected to be desorbed, at a rate given by:

$$R_{\text{cr}} = F_{\text{cr}} \langle \pi a_{\text{g}}^2 n_{\text{g}} \rangle \phi M_s(i, t) \quad \text{cm}^{-3} \text{ s}^{-1}. \quad (3)$$

where F_{cr} is the flux of cosmic rays, ϕ is an efficiency parameter such that $\phi M_s(i, t)$ is the number of molecules released per cosmic ray impact, a_{g} is the grain radius and n_{g} is the number density of grains. We have used a value for the total grain surface area per cm³, $\langle \pi a_{\text{g}}^2 n_{\text{g}} \rangle$, of $2.4 \times 10^{-22} n_{\text{H}} \text{ cm}^{-1}$, consistent with Rawlings et al. (1992) if we use a value for the depletion coefficient of ~ 1.0 .

Léger et al. (1985) showed that the iron nuclei component of cosmic rays should be the most effective in heating the grain, and therefore we adopt the value for F_{cr} of $2.06 \times 10^{-3} \text{ cm}^{-2} \text{ s}^{-1}$ which is an estimate of the

iron fraction of the canonical cosmic ray flux. It is based on the proton cosmic ray flux in the interstellar medium given by Morfill et al. (1976), and the iron to proton ratio of 1.6×10^{-4} (estimated by Léger et al. (1985)).

An estimate for ϕ can be taken from Léger et al. (1985) who worked out the evaporation rate of CO per grain resulting from both whole-grain and spot-grain heating by cosmic rays. For spot-grain heating, they calculated that 6×10^4 CO molecules would be released per cosmic ray impact, independent of grain size. For whole grain heating, however, the result was found to strongly depend on grain size, dominating spot-grain heating for $a_g \leq 2500$ Å. We have tested this mechanism with values of ϕ ranging from 10^2 to 10^6 , but we only present the results for $\phi = 10^5$ to be consistent with the lower estimate predicted by spot-grain heating. Since the volatile species make up approximately 40% of the grain mantle, using $\phi = 10^5$ implies that the number of molecules released per cosmic ray impact is $\phi M_s(i) \approx 4 \times 10^4$.

2.3 Cosmic ray induced photodesorption

As cosmic rays travel through a molecular core, they ionise and excite the absorbing gas. Prasad & Tarafdar (1983) investigated the excitation of the Lyman and Werner systems of the hydrogen molecule, caused by collisions with either primary cosmic ray particles or secondary electrons released by cosmic ray ionisation. They found that emissions resulting from these excitations may be capable of maintaining a chemically significant level of UV photon flux in the interiors of dark clouds, where the interstellar UV radiation is heavily extinguished ($A_V \geq 5$).

When a UV photon impinges upon the mantle of a grain, it is most likely to be absorbed by H₂O which may then be dissociated into H and OH (Hartquist & Williams 1990). The energy of the dissociation products cause local heating, capable of desorbing nearby molecules. This process is non-selective, and proceeds at a rate given by:

$$R_{\text{crpd}} = F_{\text{P}} \langle \pi a_g^2 n_g \rangle Y M_s(i, t) \quad \text{cm}^{-3} \text{ s}^{-1}. \quad (4)$$

where F_{P} is the photon flux and Y is the yield per photon. Prasad & Tarafdar (1983) estimated F_{P} to be just $1350 \text{ cm}^{-2} \text{ s}^{-1}$, but here we use a value of $4875 \text{ cm}^{-2} \text{ s}^{-1}$ taken from equation (21) of Cecchi-Pestellini & Aiello (1992)¹. This value is much higher than the estimate of Prasad & Tarafdar (1983) because it explicitly includes the contribution to the excitation rate of H₂ by cosmic ray protons, not just the secondary electrons. We present the results for $Y = 0.1$, as estimated by Hartquist & Williams (1990), but as this value is uncertain we also ran the model with values of Y ranging from 1×10^{-3} to 100.

Obviously, the relative importance of these mechanisms depends upon the values used for ε , ϕ and Y , which can be treated as free parameters. In this paper, we present the results for the values stated above, and in Section 6 we derive upper limits for these parameters based on observations.

¹ This is consistent with using a cosmic ray ionisation rate, ζ , of $1.3 \times 10^{-17} \text{ s}^{-1}$.

3 THE MODEL

In order to see clearly the relative importance of the various desorption mechanisms for the interstellar chemistry of molecular cores, we have used a simple one-point model of a static, isothermal dark cloud, at a density of $n_{\text{H}} = 10^5 \text{ cm}^{-3}$ and a temperature of 10 K. The core has a visual extinction, A_V , of 10 magnitudes, and a radius of ~ 0.05 pc, implying a mass of $1 M_{\odot}$.

3.1 The chemical model

The model, adapted from Viti et al. (2004), includes gas-phase reactions, freeze-out, surface reactions and desorption, with 127 gas phase and 40 mantle species. The gas phase reaction network consists of 1741 reactions from the UMIST Rate99 database (Le Teuff et al. 2000). Photoreactions are included, which take into account both the external interstellar radiation field and the internal cosmic ray induced UV field. Both direct and indirect ionisation by cosmic rays are also included, using a cosmic ray ionisation rate, ζ , of $1.3 \times 10^{-17} \text{ s}^{-1}$. The hydrogen atom abundance (that drives the H₂ formation desorption mechanism) is determined self-consistently in the chemical network. The species and reactions are taken from the model as in Viti et al. (2004), which describes the rich chemistry of hot cores. The number of species and elements should therefore be more than sufficient to describe the low mass case in this paper. Freeze-out and grain chemistry are described in Section 3.2.

The initial conditions are atomic, apart from carbon which is all singly ionised, and half the hydrogen nuclei are in the form of H₂. The initial elemental abundances are taken from Sofia & Meyer (2001).

3.2 Freeze-out and grain chemistry

The rate of accretion onto grains of species i (in $\text{cm}^{-3} \text{ s}^{-1}$) is given by (Rawlings et al. 1992):

$$\frac{dn(i)}{dt} = -4.57 \times 10^4 \langle \pi a_g^2 n_g \rangle T^{1/2} C S(i) m(i)^{-1/2} n(i) \quad (5)$$

where T is the gas temperature, $m(i)$ is the mass of species i in atomic mass units, $n(i)$ is the number density of species i , $\langle \pi a_g^2 n_g \rangle$ has the same definition as in Section 2, and $S(i)$ is the sticking coefficient of species (i). Following WRW94, we have used $S(i) = 0.3$ for all species.

C is a factor which takes into account electrostatic effects:

$$\begin{aligned} C &= 1 && \text{for neutral species} \\ &= 1 + (16.71 \times 10^{-4} / a_g T) && \text{for singly charged} \\ &&& \text{positive ions.} \end{aligned} \quad (6)$$

The only surface reactions that occur are hydrogenation of certain unsaturated species, and dissociative recombination of molecular ions. These reactions are assumed to occur instantly and the products remain on the grain surface until they are desorbed by one of the processes named above. H₂ is an exception in that it is assumed to desorb immediately because of the high exothermicity of the reaction, as is indicated by experimental studies (Creighan, Perry & Price 2006).

4 RESULTS

By comparing the rate coefficients given for each of the desorption mechanisms, if we use $\varepsilon = 0.01$, $\phi = 10^5$ and $Y = 0.1$ at a density of $n_{\text{H}} = 10^5 \text{ cm}^{-3}$, desorption via H_2 formation will dominate if the equilibrium atomic hydrogen density is greater than $\sim 0.4 \text{ cm}^{-3}$. If ε is as high as 0.1 then this mechanism will always be dominant.

Figures 1 and 2 compare the effect of the different desorption mechanisms in a static cloud at a density of 10^5 cm^{-3} for selected observable molecules. In general, desorption has the most significant effect on gas phase abundances after approximately 10^6 years, which is when the molecules begin to freeze-out. Each of the desorption mechanisms are effective enough to be able to compete with freeze-out at late times, preventing full depletion of species onto grains. The exceptions are the sulphur bearing species, H_2S and CS , whose freeze-out is only prevented by the non-selective cosmic ray photodesorption. This mechanism is also able to enhance abundances of molecules such as NH_3 and H_2S at times as early as 10^5 years. For the case of NH_3 this is because the NH_3 in the mantle builds up relatively quickly (compared to molecules like CO), so direct desorption by this mechanism can proceed close to its maximum rate. However, since the H_2 formation and direct cosmic ray heating mechanisms are not able to desorb NH_3 directly, desorption via these mechanisms can only affect NH_3 once enough NO has been desorbed to enhance the gas phase production (via the reaction $\text{NO} + \text{NH}_3^+ \rightarrow \text{NH}_3 + \text{NO}^+$).

For most of the species shown in Figures 1 and 2, desorption via H_2 formation with $\varepsilon = 0.1$ is the most effective mechanism, being able to produce equilibrium abundances up to an order of magnitude greater than the other mechanisms. However, there are several molecules (NH_3 , H_2S and CS), for which cosmic ray induced photodesorption is more effective, even though desorption via this mechanism proceeds at a rate more than ten times slower than H_2 formation with $\varepsilon = 0.1$. This is because we have assumed desorption via H_2 formation is selective, only being able to desorb molecules with adsorption energies less than 1210 K (CO , NO , N_2 , O_2 , C_2 and CH_4). Evidently, the higher gas phase abundances of these molecules caused by selective desorption do not have a significant effect on the gas phase chemistry of molecules like H_2S and CS , so their freeze-out is not prevented by selective mechanisms.

In the following subsections we look at the effectiveness of each mechanism under different conditions, by varying the density and the initial atomic hydrogen density. We also discuss further the effects of selectivity in Section 4.3.

4.1 Varying the density

When the model was run at a density of $n_{\text{H}} = 10^6 \text{ cm}^{-3}$, it was found that the equilibrium abundances of the desorbed species were reduced approximately by a factor of 10 compared to the equivalent runs at 10^5 cm^{-3} . Given that $n(\text{H})$ and M_{s} appear to show little variation in their equilibrium values at different densities, the rates for each desorption mechanism should not depend on density. However, the rate for freeze-out has a direct linear dependence on density, so it is expected that the equilibrium abundances of desorbed

species should scale roughly as n_{H}^{-1} , which would explain the reduction in equilibrium abundances found in the results.

4.2 Varying the initial atomic hydrogen density

Since desorption via H_2 formation depends on the abundance of atomic hydrogen, it would be expected that varying the initial ratio of atomic to molecular hydrogen could also influence how efficient this mechanism is. However, even when the model was run with all hydrogen in the form of H_2 initially, after 10^5 years the abundance of atomic hydrogen had reached the same value ($n(\text{H}) \sim 0.4 \text{ cm}^{-3}$) as in the previous runs (which had only half the hydrogen nuclei in H_2 initially), so there was no noticeable difference in the desorption via H_2 formation rate.

4.3 Varying the threshold adsorption energy for selective mechanisms

So far we have assumed that the selective desorption mechanisms (H_2 formation and direct cosmic ray heating) are only capable of desorbing molecules with adsorption energies less than or equal to the value $E_{\text{t}} = 1210 \text{ K}$. This number was chosen to be consistent with the study by WRW94, who assumed that only CO , N_2 , C_2 , O_2 and NO could be desorbed by these processes. CH_4 also has an adsorption energy of less than 1210 K, so we have also included CH_4 as a ‘volatile’ species. Although Léger et al. (1985) calculated that mantles composed *purely* of refractory ices such as CO_2 , H_2CO , HCN , NH_3 and H_2O are unlikely to be affected by these mechanisms, they predicted that if these molecules are mixed with volatile species then spot heating processes may be able to raise the temperature of the grains enough to desorb these refractory molecules. Since the H_2 formation and direct cosmic ray heating mechanisms are both capable of spot-heating, we thought it was necessary to investigate the effect of varying E_{t} .

Figures 3 and 4 show the effect of varying E_{t} for the H_2 formation mechanism with $\varepsilon = 0.01$. The adsorption energies for each mantle species were taken from Aikawa et al. (1997), apart from H_2O which was taken from Fraser et al. (2001). Some of the molecules, such as CO , CH_4 and H_2CO are relatively unaffected, even when E_{t} is so high (10 000 K) that all molecules can be desorbed. In the case of H_2CO which has an adsorption energy of 1760 K (Aikawa et al. 1997) this may seem rather surprising. The behaviour can be explained by the fact that, for the model and parameters that we have considered, gas-phase formation of H_2CO (via $\text{CH}_3 + \text{O}$) dominates over desorption. On the other hand, molecules such as NH_3 and HCN show differences in abundances of more than one order of magnitude when they reach equilibrium. These differences can be explained as follows:

- (i) NH_3 : The equilibrium fractional abundance of NH_3 increases from 1.4×10^{-9} to 2.5×10^{-8} when E_{t} increases from 3000 K to 4000 K. This change is simply because the adsorption energy of NH_3 is 3080 K, so for $E_{\text{t}} \geq 4000 \text{ K}$, NH_3 can be desorbed directly. For $E_{\text{t}} \leq 4000 \text{ K}$, the main production of NH_3 is through the reaction $\text{NH}_3^+ + \text{NO} \rightarrow \text{NO}^+ + \text{NH}_3$.
- (ii) HCN : The equilibrium fractional abundance of HCN increases from 9.5×10^{-11} to 2.0×10^{-9} when E_{t} increases

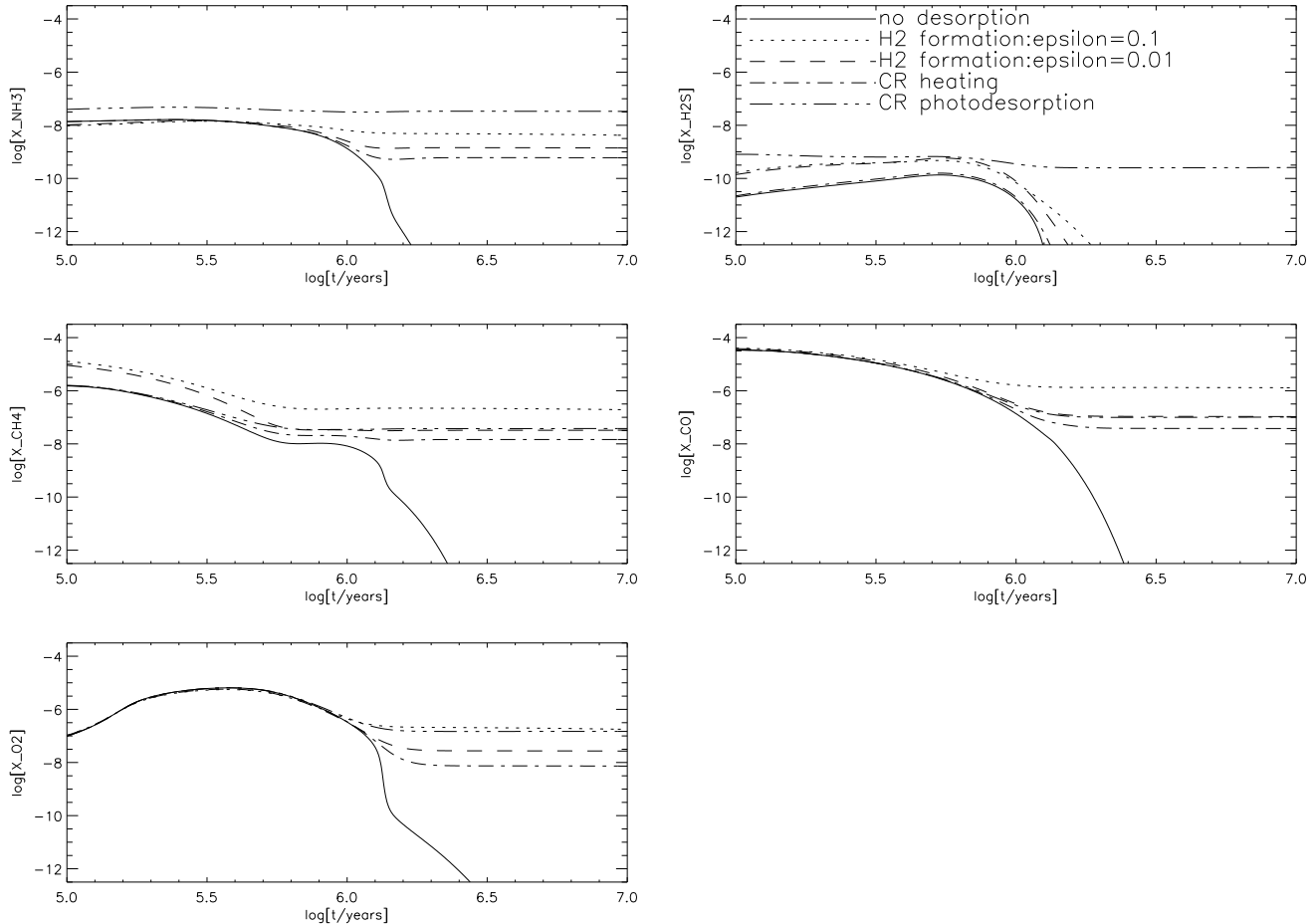


Figure 1. The time evolution of the molecules NH_3 , H_2S , CH_4 , CO and O_2 in a static cloud of density $n_{\text{H}} = 10^5 \text{ cm}^{-3}$, $T = 10 \text{ K}$, at a point with $A_V = 10 \text{ mag}$. The abundances of species relative to hydrogen are shown as a function of time in years. The different curves compare the evolution of the species with no desorption, desorption via H_2 formation with $\varepsilon = 0.1$ and 0.01 , desorption via direct cosmic ray heating and cosmic ray photodesorption (see key).

from 3000 K to 4000 K. The adsorption energy of HCN is actually greater than 4000 K, so this is not a consequence of direct HCN desorption. In fact, it is the direct desorption of NH_3 that produces the HCN via the reaction $\text{NH}_3 + \text{CN} \rightarrow \text{HCN} + \text{NH}_2$ when E_t is greater than 4000 K. Below this energy, the main route of production of HCN is the reaction $\text{H} + \text{H}_2\text{CN} \rightarrow \text{HCN} + \text{H}_2$.

For CS and H_2S , freeze-out is only prevented if E_t is greater than 2000 K. This is because at this energy both CS and H_2S can be directly desorbed. For CS if E_t is increased further from 2000 K to 3000 K, the equilibrium abundance of CS increases again by approximately an order of magnitude. This is due to the direct desorption of H_2CS at 2250 K, which can increase the CS abundance through the reaction $\text{C}^+ + \text{H}_2\text{CS} \rightarrow \text{CS} + \text{CH}_2^+$.

5 COMPARISON WITH EXISTING MODELS AND FORMULATIONS

We first of all compare our results to those of WRW94, which is the closest previous study to our own, then we

consider two other studies, Willacy & Millar (1998) and Hartquist & Williams (1990) (hereafter WM98 and HW90 respectively), whose conclusions differed to ours. We also discuss various assumptions that are made in most chemical models of molecular clouds in which desorption is included, with particular reference to the formulation of desorption by direct cosmic ray heating by HH93.

5.1 Comparison to WRW94

WRW94 investigated each of the desorption mechanisms discussed above, in the case of a collapsing cloud. They concluded that the only significant mechanism was desorption arising from H_2 formation on grains if it was assumed to be non-selective, using values for ε of 0.1 and 0.8. Since we have found that, for a static cloud, all desorption mechanisms are significant and can prevent complete freeze-out, it is therefore worth checking that our model agrees with that of WRW94 when it is run under similar conditions.

To simulate a collapse, as in WRW94, we have used a spherically symmetric, isothermal model, undergoing a free-fall collapse. The collapse is modified by a retardation factor

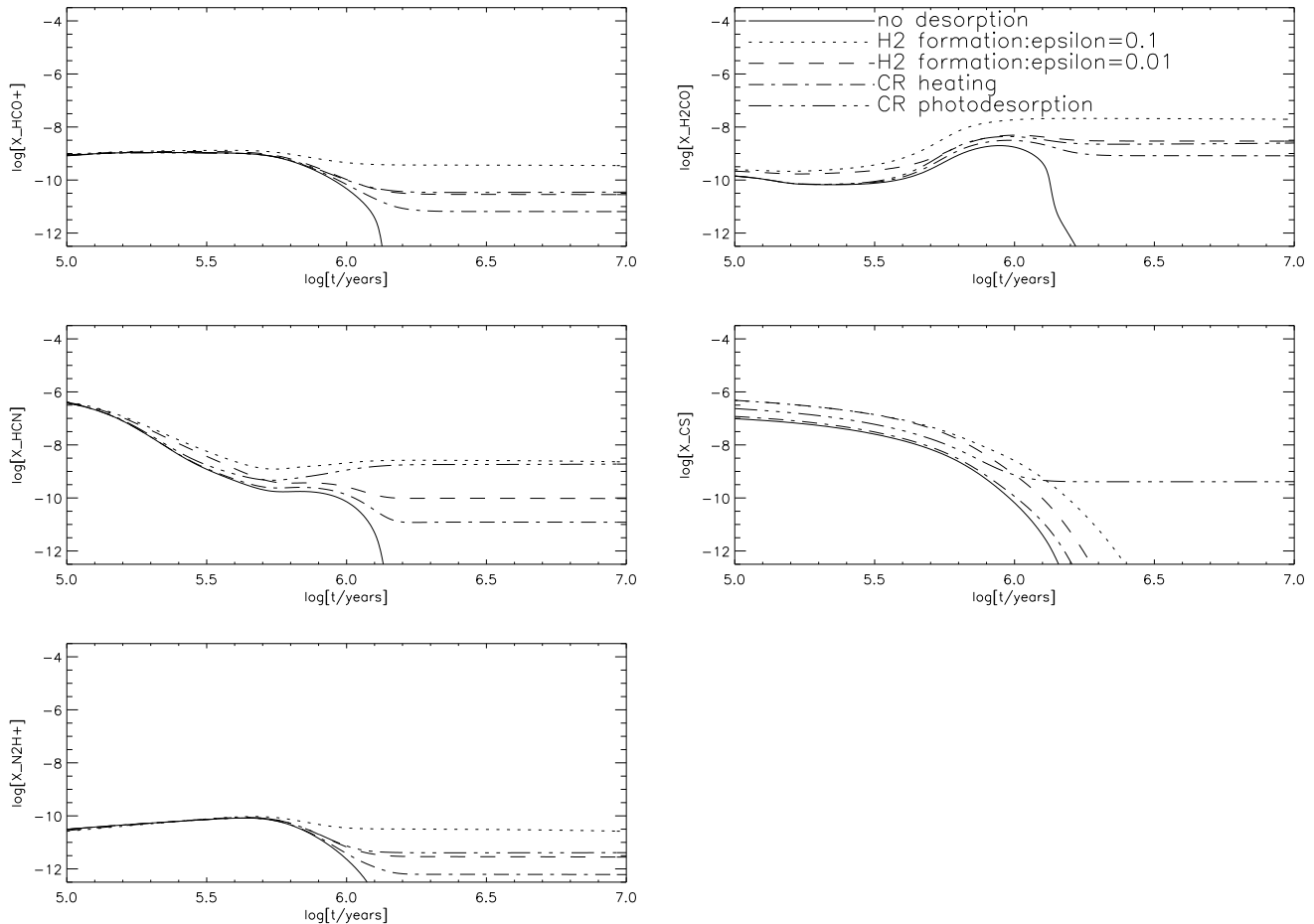


Figure 2. As in Figure 1 but for the molecules HCO^+ , H_2CO , HCN , CS and N_2H^+ .

B due to magnetic fields and other factors (Rawlings et al. 1992). WRW94 used $B = 0.7$, a temperature of 10 K, an initial density, n_0 , of $3 \times 10^3 \text{ cm}^{-3}$ and a final density of 10^6 cm^{-3} . The initial visual extinction of the cloud was 4.4 magnitudes. Figure 5 shows the results from our model when it was run with these parameters. We have plotted the abundances of the same molecules that appear in Figure 1 of WRW94, and have converted time to radius as they did to allow for easy comparison between our results and theirs. Even though the chemical reaction network in our model is much more complicated than in the WRW94 model, both models agree that desorption has the greatest effect on NH_3 and HCN . Also, under these conditions, we agree that the other mechanisms (direct cosmic ray heating and cosmic ray photodesorption) do not significantly affect the abundances of these molecules.

5.2 Comparison to WM98

WM98 carried out an investigation in which they tested the three desorption mechanisms used in our model, as well desorption by the explosive chemical reactions of radicals. Their model used similar physical conditions to ours, except that they adopted a lower density ($n_{\text{H}} = 2 \times 10^4 \text{ cm}^{-3}$). They found that models that include desorption by H_2 formation

(with values of ϵ ranging from 0.1 to 1.0) gave the best agreement to the observed gas phase abundances in TMC-1.

This actually agrees well with our model, since we also find that desorption by H_2 formation with $\epsilon = 0.1$ is the most efficient mechanism. WM98 concluded, however, that desorption by direct cosmic ray heating and cosmic ray photodesorption were too inefficient because they generally under-predicted the gas phase abundances. Thus, for example, CO , was found to be underabundant by approximately two orders of magnitude at an age of 5 Myr using the cosmic ray induced mechanisms. We agree that, when comparing the desorption mechanisms using our standard values of ϵ , ϕ and Y , desorption by H_2 formation can indeed maintain gas-phase abundances up to two orders of magnitude higher than the other mechanisms. But, since these parameters are so uncertain, we believe it is too early to confidently rule out cosmic ray heating and cosmic ray photodesorption as important desorption mechanisms.

5.3 Comparison to HW90

In their study, Hartquist & Williams (1990) carried out a purely theoretical analysis of cosmic ray induced desorption. They argued that direct cosmic ray heating would not be able to maintain significant gas-phase CO abundances be-

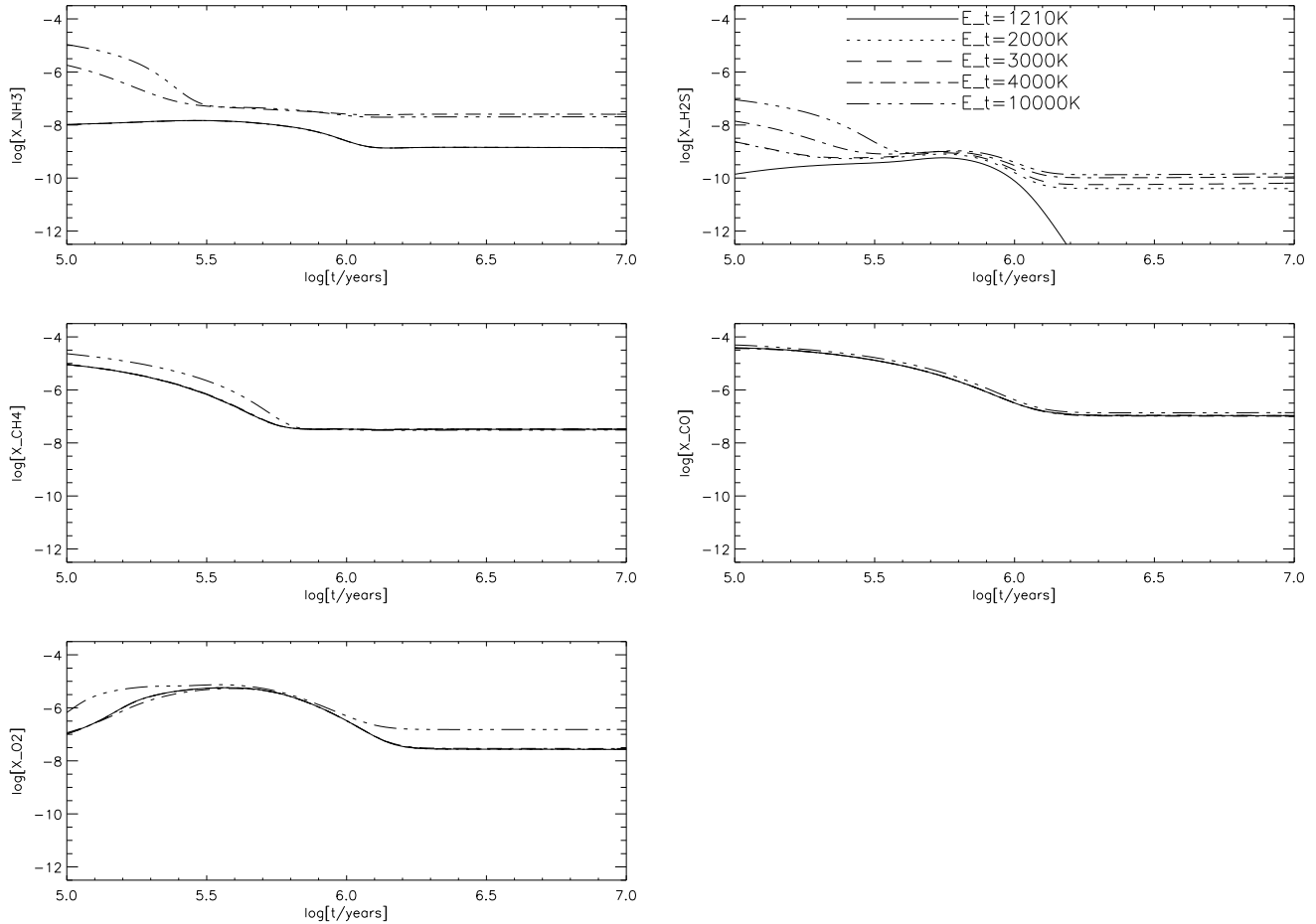
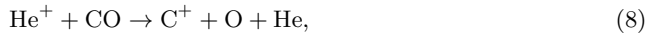


Figure 3. The effect of varying E_t for desorption via H_2 formation with $\varepsilon = 0.01$, in a static cloud of density $n_H = 10^5 \text{ cm}^{-3}$ at 10 K, for the molecules NH_3 , H_2S , CH_4 , CO and O_2

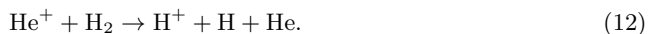
cause the desorbed CO would be destroyed by reactions with He^+ (leading to the formation of hydrocarbons). Their analytical calculation of the gas-phase CO abundance at high densities gives the result

$$n_g(CO) \propto e^{-\beta t}, \quad (7)$$

where β depends on the rates of the reactions



and



Reactions (8) to (10) are the main formation and destruction routes for CO , with reactions (8) and (10) referring to the freeze-out and desorption of CO . Reactions (11) and (12) are assumed to be the main formation and destruction routes of He^+ at high densities.

Hartquist & Williams (1990) calculated β to be

$$\beta^{-1} \approx 3 \times 10^6 \text{ yr} (n_H / 10^6 \text{ cm}^{-3}). \quad (13)$$

However, when we redo the calculation with the (updated) rate coefficients for these reactions used in our model, we obtain values of β^{-1} that are a factor almost six orders of magnitude larger. This implies that significant gas-phase CO abundances can be maintained over the lifetime of a typical cloud. The difference arises because we have used a much smaller desorption rate for CO (given by equation (3)). So, in fact, using a *smaller* desorption rate allows for a more controlled release of CO into the gas phase and thus enables the CO to remain in the gas-phase for a longer period of time.

Hartquist & Williams (1990) also concluded that cosmic ray induced photodesorption would only be effective in regions where the number density is 10^3 cm^{-3} or lower. They calculated the ratio at which heavy molecules desorb by cosmic ray induced photodesorption to the rate at which they freeze-out to be

$$R \approx \left(\frac{X_Z}{10^{-7}} \right)^{-1} \left(\frac{n_H}{10^5 \text{ cm}^{-3}} \right)^{-1} \left(\frac{\zeta}{10^{-17} \text{ s}^{-1}} \right), \quad (14)$$

where X_Z is the fractional abundance of heavy molecules in the gas phase and ζ is the cosmic ray ionisation rate. This expression implies that cosmic ray photodesorption will be more efficient at low densities. The rates we have used are

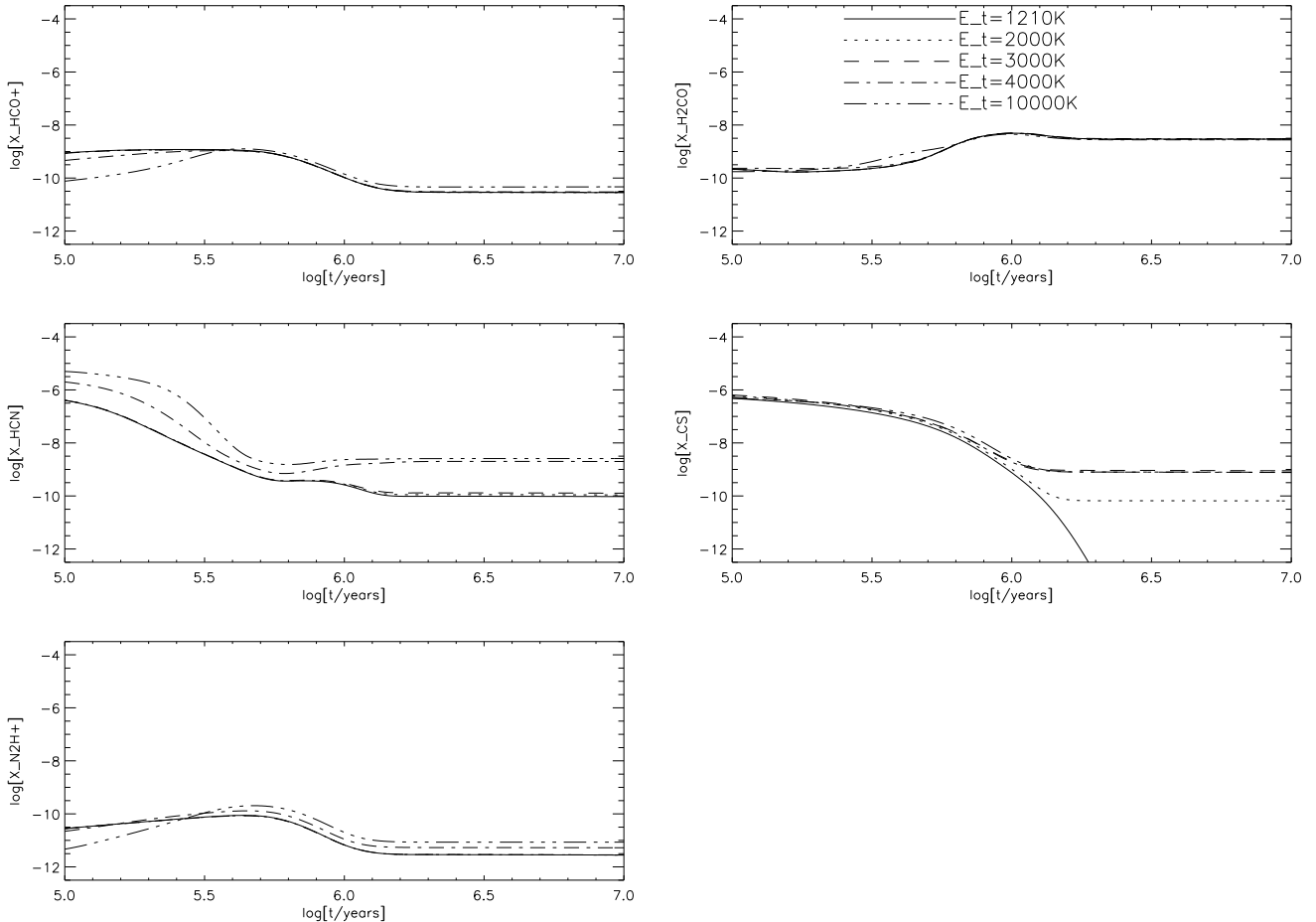


Figure 4. As in figure 3 but for the molecules HCO^+ , H_2CO , HCN , CS and N_2H^+

consistent with this ratio, but our results clearly indicate that the cosmic ray induced photodesorption mechanism can still maintain significant gas phase abundances of heavy molecules at densities as high as 10^5 cm^{-3} , even though the efficiency of the process is not at its peak at this density.

5.4 Discussion of other formulations and assumptions

As mentioned earlier, other previous models that have included desorption in dark ray clouds tend to only include desorption by direct cosmic ray heating. One of the most commonly used formulations is that of HH93, who assumed that classical ($\sim 0.1 \mu\text{m}$) grains are impulsively heated by relativistic nuclei with energies 20-70 MeV, depositing an average of 0.4 MeV per impact, raising the local (hot spot) temperature of the grain to 70 K. The subsequent (thermal) desorption rate is then calculated from the binding energies of the various molecular species and the cooling profile of the dust grain. In practice, the details of the cooling are simplified to a ‘duty cycle’ approach, so the desorption rate is proportional to the fraction of time spent by the grains in the vicinity of 70 K, $f(70 \text{ K}) \sim 3.16 \times 10^{-19}$. The rate coefficient is then given by:

$$k_{\text{cr-HH93}}(i) = f(70 \text{ K})\nu_0(i) \exp[-E_a(i)/70 \text{ K}] \text{ s}^{-1} \quad (15)$$

where $\nu_0(i)$ and $E_a(i)$ are the characteristic adsorbate vibrational frequency and adsorption energy for species i respectively.

Flower et al. (2005) formulated a similar (but simpler) rate for cosmic ray desorption (in $\text{cm}^{-3}\text{s}^{-1}$) given by:

$$R_{\text{crd-FPW05}} = M_s(i) \langle \pi a_g^2 n_g \rangle \gamma \exp \left[\frac{-(E_a(i) - E_a(\text{CO}))}{70 \text{ K}} \right] \quad (16)$$

where $\gamma = 70 \text{ cm}^{-2} \text{ s}^{-1}$ gives the desorption rate of CO per unit area of dust grains as derived by Léger et al. (1985). This factor takes into account the cosmic ray flux, F_{cr} , and the efficiency parameter, ϕ , which were explicitly included in our rate. The above rate includes the same exponential factor as in HH93, but does not take into account variations in ν_0 for each species.

We decided not to use the above formulations because, bearing in mind the exponential sensitivity of the desorption rate to the ratio of the hot spot temperature to the binding energy, the resulting rates are extremely uncertain and strongly dependent on a number of very poorly constrained free parameters including the grain size and morphology, the molecular binding energies, the rate and energy/mass spectrum of the cosmic rays.

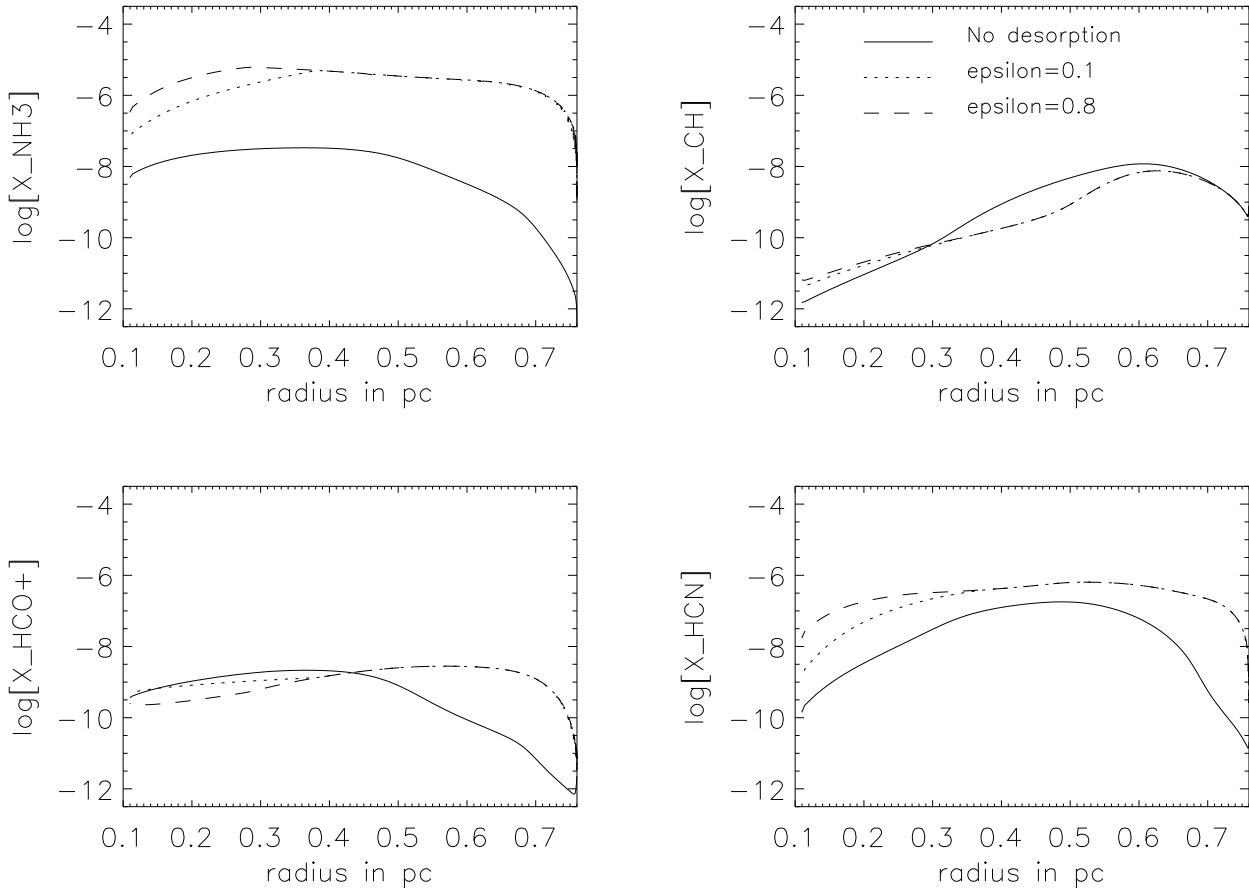


Figure 5. The variation of NH_3 , CH , HCO^+ and HCN with radius for a cloud collapsing from $n_{\text{H}} = 3 \times 10^3 \text{ cm}^{-3}$ to 10^6 cm^{-3} at 10 K including non-selective desorption resulting from H_2 formation, as in Figure 1 of Willacy et al. (1994b)

We can examine a few of these assumptions in a little more detail:

(i) The formulations given above assume that interstellar dust grains can be thought of as homogeneous, symmetrical (spherical, spheroidal, or cylindrical) entities. In reality, we know that the grains may have very complex morphologies (‘fluffy aggregates’) with non-uniform thermal properties and composition. We can speculate that these grains therefore consist of poorly thermally connected sub-units, so that both the spot-heating and the whole grain heating rates may be quite different to what is derived for spherical, uniform dust grains.

(ii) Most of these studies also only consider the gas-grain interactions with large ($\sim 0.1 \mu\text{m}$), classical grains. The justification given for this is that the equilibrium temperature of the (cosmic ray heated) smaller grains is too high to allow gas-phase species to freeze-out. However, this differentiation is not apparent in Léger et al. (1985) and there is no direct observational evidence of the universal presence of a population of warm dust grains. The smaller grains present a much larger surface area per unit volume of gas than the classical grains, so this is an important issue.

(iii) Concerning the desorption process itself, the assump-

tion is usually made that the mantle ice is pure, so that the adopted binding/desorption energies correspond to the pure substance. Real ices are likely to have complex compositions and temperature-dependent morphologies. Laboratory work (Collings et al. 2003, 2004) shows that the desorption characteristics are drastically modified in such circumstances in a way that is very species-dependent. Thus, for example, in a mixed $\text{CO}/\text{H}_2\text{O}$ ice, CO is desorbed in four distinct temperature bands (with $T \sim 25 - 100 \text{ K}$).

(iv) Bringa & Johnson (2004) performed detailed molecular dynamics calculations of the thermal evaporation process driven by a cylindrical heat pulse, concentrating on a classical grain of $\sim 0.1 \mu\text{m}$, heated by a heavy cosmic ray ion. Even with the assumption of a single desorption energy/threshold for each species they still obtained very different results to HH93 – most notably the derived H_2O and CO desorption rates were found to be an order of magnitude higher and lower, respectively, as compared to HH93. However, even here, the calculations make very general assumptions about the cosmic ray energy spectrum and adopt a spherically symmetric grain with uniform thermal properties.

(v) The issue of the surface chemistry is often not considered in many of the chemical models which use these des-

orption formulations. This would only be valid if one makes the seemingly unreasonable assumption that the surface residence timescale of adsorbed species is less than the surface migration timescale for reactive species such as hydrogen atoms.

Because of these various uncertainties we must conclude that although approximate quantifications of the rate of desorption driven by cosmic ray grain heating are useful, the numerical details are very poorly constrained and anything more complicated or specific than our simple approach is very hard to justify.

The most important conclusion of this section, therefore, is that due to the considerable uncertainties in the microphysics of ice desorption which are, as yet, very poorly constrained by laboratory and/or theoretical studies, it is very difficult to make *qualitative* distinctions between different desorption mechanisms: Each of the desorption models discussed above has its own merits, but that there is insufficient information to discriminate or validate these models. However, we also make the point that, through empirically deduced values of the depletions, we *can* make well-constrained *quantitative* estimates of the desorption efficiencies. In the next section, we compare our models to observational results. Thus, by consideration of the deduced desorption efficiencies we are able to comment on the allowed values of the free parameter in each of the desorption models (ε , ϕ or Y) that are consistent with the observations.

6 COMPARISON WITH OBSERVATIONS

As a consequence of our poor understanding of the theory of ice desorption, it is proposed that, rather than using desorption efficiencies as an input to the chemical models we invert the process and use whatever observations we can safely interpret to constrain, empirically, the nature and efficiencies of the desorption processes. We can then use that information to predict the chemical behaviours of other species and generate physical diagnostic indicators of the molecular clouds.

Observations of CO isotopomers in several pre-stellar cores provide strong evidence for the depletion of CO onto grains. For example, Redman et al. (2002) were able to estimate that at least 90 % of CO is depleted within 5000 AU of the centre of the pre-stellar core L1689B, by comparing their observations of the $C^{17}O$ $J = 2 \rightarrow 1$ line with models which included CO depletion in the centre of the core. Since L1689B is a typical pre-stellar core with a density of $n_H = 1.2 - 1.4 \times 10^5 \text{ cm}^{-3}$ (Bacmann et al. 2000), it is an ideal candidate with which we can compare our results.

CO depletion has also been estimated in several other pre-stellar cores, such as L1544, L1709A, L310, L328, L429 and Oph D (Bacmann et al. 2002). In these cases, the CO depletion is estimated by comparing the observed ratio, X , of the $C^{17}O$ and H_2 column densities, to the ‘canonical’ abundance determined by Frerking et al. (1982) towards dark cores, $X_{\text{can}} = 4.8 \times 10^{-8}$. The CO depletion factor, f , is defined by X_{can}/X , and was found to vary from 4.5 (in L1689B, which appears to be slightly less than the depletion estimated by Redman et al. (2002)) to 15.5 in L429. Since X_{can} is the value of X obtained in undepleted conditions, and assuming that there is no selective depletion of different

isotopomers of CO (so the fraction of $C^{17}O$ depleted onto grains is the same as the fraction of total CO depleted), then the fraction of CO depleted onto grains is given by $1 - 1/f$. This implies that CO depletion ranges from 78% to 94% in these cores. The densities of these cores are all of order $n(H_2) = 10^5 \text{ cm}^{-3}$ so it is also worth comparing these depletion fractions to our model.

Although our results have indicated that including desorption inhibits full freeze-out allowing abundances to reach an equilibrium, the percentage of CO frozen-out onto grains is actually greater than 98% ($f = 50$) for all of the mechanisms investigated, which is consistent with the observations above.

If we assume that L1689B is in a state of equilibrium, the values of ε , ϕ and Y needed to give the 90% freeze-out estimated in L1689B are approximately 0.5, 1.3×10^7 and 5.5 respectively. We calculated these values by assuming that freeze-out and desorption of CO are the main processes governing the CO abundance, so by equating these rates with 90% of CO on the grains and 10% remaining in the gas phase we can predict the efficiencies needed. We then ran the model with these values of ε , ϕ and Y to confirm that the observed CO depletion is obtained. Since it is possible that L1689B is not in equilibrium and further freeze-out could be achieved, this gives us an upper limit for these parameters.

If we use the values estimated by Bacmann et al. (2002), for L1689B (in which they deduce that CO is depleted by 78%) we obtain even higher limits for ε , ϕ and Y of 1.4, 3.3×10^7 and 14.0 respectively. For L429, in which a CO depletion of 94% was deduced, the values for ε , ϕ and Y are reduced to 0.31, 7.5×10^6 and 3.2 respectively. The values for all the other cores studied by Bacmann et al. (2002) would lie in between the values for L1689B and L429.

These values are much higher than the estimates used in our model, indicating that if these desorption mechanisms operate then they are very efficient. However, using these observations it is not possible to determine which of the mechanisms is operating, or if it is a combination of all three.

7 CONCLUSIONS

There are two major conclusions from this study: Firstly, we have shown that the usual assumption that cosmic ray desorption is the most effective desorption mechanism in dark molecular clouds is not always valid. All three desorption mechanisms that we have considered (desorption via H_2 formation on grain surfaces, direct cosmic ray heating and cosmic ray photodesorption) have been shown to have significant effects on the gas phase abundances in quiescent dark molecular clouds and so should not be neglected in chemical models. These processes all operate on timescales of the order of $\sim 10^6$ years. Each of the processes is capable of preventing total freeze-out, but in an equilibrium quiescent dark cloud of density 10^5 cm^{-3} , the predicted percentage of freeze-out is always greater than 98%. This figure is in good agreement with the observations (e.g. L1689B).

Addressing the specifics of the desorption processes, desorption via H_2 formation, if it is efficient ($\varepsilon = 0.1$), is the most effective mechanism. However the complete freeze-out of some species, such as CS and H_2S , can only be prevented by the cosmic ray photodesorption mechanism, which is non-

selective. The relative importance of the three mechanisms appear to be insensitive to variations in the density and the initial atomic to molecular hydrogen ratio. For the selective desorption mechanisms, choosing the threshold adsorption energy, E_t , (such that molecules with adsorption energies less than E_t will be desorbed), can have a strong effect on the chemistry, particularly on molecules such as NH_3 , HCN , CS and H_2S .

Secondly, our understandings of the chemical and physical structure of dust grains and the physical processes which drive desorption are, as yet, very incomplete and a purely theoretical approach to the problem is inadvisable. In this study we have investigated three particular desorption mechanisms (desorption via H_2 formation, direct cosmic ray heating and cosmic ray photodesorption) and have used the observed molecular depletions to constrain the poorly-determined free parameters in desorption processes. This is the first attempt at an empirical determination of the desorption efficiencies. Bearing in mind the huge uncertainties in these efficiencies, this empirical approach is the one that we recommend for use in future studies of interstellar chemistry where gas-grain interactions play an important role.

ACKNOWLEDGEMENTS

JFR is supported by a PPARC studentship.

REFERENCES

- Aikawa Y., Umebayashi T., Nakano T., Miyama S.M., 1997, *ApJ*, 486, 51
- Allen M., Robinson G.W., 1975, *ApJ*, 195, 81
- Bacmann A., André P., Puget J-L., Abergel A., Bontemps S., Ward-Thompson D., 2000, *A&A*, 361, 555
- Bacmann A., Lefloch B., Ceccarelli C., Castets A., Steinacker J., Loinard L., 2002, *A&A*, 389, L6
- Bringa E.M., Johnson R.E., 2004, *ApJ*, 603, 159
- Cecchi-Pestellini C., Aiello S., 1992, *MNRAS*, 258, 125
- Creighan S.C., Perry J.S.A., Price S.D., 2006, *JChemPhys*, 124, art. no 114701
- Collings, M.P., Dever, J.W., Fraser, H.J., McCoustra, M.R.S., 2003, *ApJ*, 583, 1058
- Collings, M.P., Anderson, M.A., Chen, R., Dever, J.W., Viti, S., Williams, D.A., McCoustra, M.R.S., 2004, *Mon. Not. R. Astron. Soc.*, 354, 1133
- Duley W.W., Jones A.P., Whittet D.C.B., Williams D.A., 1989, *MNRAS*, 241, 697
- Duley, W.W., Williams, D.A., 1993, *Mon. Not. R. Astron. Soc.*, 260, 37
- Evans N.J., Rawlings J.M.C., Shirley Y.L., Mundy L.G., 2001, *ApJ*, 557, 193
- Flower D.R., Pineau des Forêts G., Walmsley C.M., 2005, *A&A*, 436, 933
- Fraser H.J., Collings M.P., McCoustra M.R.S., Williams D.A., 2001, *MNRAS*, 327, 1165
- Frerking M.A., Langer W.D., Wilson R.W., 1982, *ApJ*, 262, 590
- Garrod, R.T., Williams, D.A., Rawlings, J.M.C., 2006, *ApJ*, 638, 827
- Garrod R.T., Wakelam V., Herbst E., 2007, *A&A*, 467, 1103
- Hartquist T.W., Williams D.A., 1990, *MNRAS*, 247, 343 (HW90)
- Hasegawa T.I., Herbst E., 1993, *MNRAS*, 261, 83 (HH93)
- Léger A., Jura M., Omont A., 1985, *A&A*, 144, 147
- Le Teuff Y.H., Millar T.J., Markwick A.J., 2000, *A&AS*, 146, 157
- Lee J-E., Evans N.J., Shirley Y.L., Tatematsu K., 2003, *ApJ*, 583, 789
- Morfill G.E., Volk H.J., Lee M.A., 1976, *J. Geophys. Res.*, 81, 5841
- Prasad S.S., Tarafdar S.P., 1983, *ApJ*, 267, 603
- Rawlings J.M.C., Hartquist T.W., Menten K.M., Williams D.A., 1992, *MNRAS*, 255, 471
- Redman M.P., Rawlings J.M.C., Nutter D.J., Ward-Thompson D., Williams D.A., 2002, *MNRAS*, 337, L17
- Roberts H., Herbst E., Millar T.J., 2004, *A&A*, 424, 905
- Ruffle D.P., Herbst E., 2000, *MNRAS*, 319, 837
- Shalabiea O.M., Greenberg J.M., 1994, *A&A*, 290, 266
- Shen C.J., Greenberg J.M., Schutte W.A., van Dishoeck E.F., 2004, *A&A*, 415, 203
- Smith I.W.M., Herbst E., Chang Q., 2004, *MNRAS*, 350, 323
- Sofia U.J., Meyer D.M., 2001, *ApJ*, 554, L221
- Viti S., Collings M.P., Dever J.W., McCoustra M.R.S., Williams D.A., 2004, *MNRAS*, 354, 1141
- Wakelam V., Herbst E., Selsis F., 2006, *A&A*, 451, 551
- Willacy K., Williams D.A., Duley W.W., 1994a, *MNRAS*, 267, 949
- Willacy K., Rawlings J.M.C., Williams D.A., 1994b, *MNRAS*, 269, 921 (WRW94)
- Willacy K., Millar T.J., 1998, *MNRAS*, 298, 562 (WM98)

This paper has been typeset from a $\text{\TeX}/\text{\LaTeX}$ file prepared by the author.